M. J. Sienko, *Appl. Phys. Lett.*, **36**, 701 (1980).
8. L. F. Schneemeyer and M. S. Wrighton, *J. Am. Chem. Soc.*, Submitted.
9. F.-R. F. Fan, H. S. White, B. Wheeler, and A. J. Bard, *J. Am. Chem. Soc.*, **102**, 5142 (1980); *This Journal*, **127**, 518 (1980).
10. H. J. Lewerenz, A. Heller, and F. J. DiSalvo, *J. Am. Chem. Soc.*, **102**, 1877 (1980).
11. W. Kautek, H. Gerischer, and H. Tributsch, *Ber. Bunsenges. Phys. Chem.*, **83**, 1000 (1979).
12. N. E. Tokel-Takvoryan, R. E. Hemingway, and A. J. Bard, *J. Am. Chem. Soc.*, **95**, 6582 (1973).
13. S. N. Frank, A. J. Bard, and A. Ledwith, *This Journal*, **122**, 898 (1975).
14. A. R. Beal, W. Y. Liang, and H. P. Hughes, *J. Phys. C*, **9**, 2449 (1976).
15. S. M. Ahmed and H. Gerischer, *Electrochim. Acta*, **24**, 705 (1979).
16. G. Nagasubramanian and A. J. Bard, *This Journal*, **128**, 1055 (1981).

Semiconductor Electrodes

XXXIV. Photoelectrochemistry of p-Type WSe_2 in Acetonitrile and the p-WSe_2-Nitrobenzene Cell

G. Nagasubramanian and Allen J. Bard*

Department of Chemistry, University of Texas at Austin, Austin, Texas 78712

ABSTRACT

The photoelectrochemical behavior of p-type WSe_2 single crystal electrodes in acetonitrile solutions containing a number of redox couples [*e.g.*, N,N,N',N'-tetramethyl-p-phenylene diamine (+ 1/0), methyl viologen (+ 2/+1), nitrobenzene (0/−1), phthalonitrile (0/−1)] was investigated. For couples with potentials in the bandgap region (*ca.* −0.4 to +1.0V *vs.* SCE), a linear increase of the photopotential with V_{redox} was observed. Couples located at more negative potentials (*i.e.*, above the conduction bandedge) also showed a photoeffect, with the photopotential pinned at ~ −0.95V; this was ascribed to surface state pinning or inversion. A PEC cell of the form p-WSe_2/$PhNO_2$, MeCN/Pt is described. Treatment of the p-WSe_2 electrode with iodide was shown to improve the efficiency of such cells.

In the preceding paper, the behavior of n-type WSe_2 in acetonitrile (MeCN) solutions was discussed (1). WSe_2 and other layer-type semiconductor materials, first proposed by Tributsch for photoelectrochemical (PEC) applications (2), have been extensively investigated recently (3-8). The results with n-WSe_2/MeCN were consistent with a flatband potential of ~ −0.3V *vs.* SCE and the existence of surface states which provide sites for surface recombination and lead to Fermi level pinning. Studies of p-type WSe_2 in MeCN were undertaken to confirm the location of the bandedges in WSe_2 and to ascertain if the behavior of a number of redox couples at this material was consistent with a pinning model.

A second goal of this work was the construction of a PEC cell for conversion of solar to electrical energy utilizing this material. Past research involving PEC cells in nonaqueous solvents such as MeCN have shown that while high stability can often be attained in such systems, the maximum light intensities that can be utilized are often limited by the low concentrations of the electroactive materials in the solution (9). However, nitrobenzene ($PhNO_2$) is miscible in all proportions with MeCN and should be a reasonable oxidant at a p-type semiconductor electrode. Cells with p-WSe_2 and $PhNO_2$ which appear stable and show monochromatic efficiencies ~4% are described here.

Experimental

Chemicals.—Nitrobenzene ($PhNO_2$) was purified following the procedure of Marcoux *et al.* (10). $PhNO_2$ was first passed through an activated alumina column and then vacuum distilled. MeCN was purified as previously described (11). The other redox couples were purified by recrystallization. All compounds were stored inside a helium-filled Vacuum Atmosphere Corporation (Hawthorne, California) glove box. Polarographic grade, tetra-n-butyl ammonium perchlorate (TBAP), dissolved and recrystallized from ethanol, thrice, and dried under vacuum ($<10^{-5}$ Torr) for 3 days was used as supporting electrolyte. The cell employed was a conventional single compartment cell of 25 ml capacity containing the p-WSe_2, a Pt working and counterelectrode and a quasi-reference electrode, which was an Ag wire immersed inside the solution and separated from it by a medium-porosity glass frit. The potential of this electrode was checked against an aqueous saturated calomel electrode (SCE) at regular intervals and was found to be constant. All potentials, unless specified otherwise, are given in V *vs.* SCE.

The p-WSe_2 single crystal generously donated by Dr. B. Miller and Dr. F. DiSalvo, Bell Laboratories, was used as the electrode. This was selected, after carefully verifying under microscope that the surface was quite free of exposed edges. A clean new crystal surface ($\perp$ C-axis) was produced by attaching adhesive tape and peeling off the surface layer. Gold was electroplated on one side of the pellet and the contact was found to be ohmic. A copper wire lead for electrical contact was attached to the gold-coated side with silver epoxy cement (Allied Product Corporation, New Haven, Connecticut) and was subsequently covered with 5 min epoxy cement. The assembly was mounted into 7 mm diam glass tubing and was held in position with silicone rubber sealant (Dow Corning Corporation, Midland, Michigan), which also served as an effective seal against the seepage of electrolyte solution to the rear of the semiconductor electrode. The exposed area of p-WSe_2 was 0.05 cm^2. The surface of the electrode was etched before use with 12M HCl for 5-10 sec and then rinsed thoroughly with distilled water and dried. The area of the Pt cylindrical wire, used as a counterelectrode, was 0.15 cm^2.

* Electrochemical Society Active Member.
Key words: capacitance, voltammetry, solar cells.

A Princeton Applied Research (PAR) Model 173 potentiostat and PAR Model 175 Universal programmer were used in all experiments, with positive feedback *iR*-compensation employed to compensate for solution resistance and internal resistance of the electrode. The *i-V* curves were recorded on a Model 2000 X-Y recorder (Houston Instruments, Austin, Texas). In solar cell experiments, the photovoltage and photocurrent between the working electrode and counterelectrode as a function of load resistance were measured with a Keithley Model 179 TRMS Digital Multimeter. The light sources were an Oriel Corporation (Stamford, Connecticut) 450W xenon lamp and a 2-mW spectrophysics Model 132 He-Ne laser. Differential capacitance was measured with PAR Model HR8 lock-in amplifier. All of the solutions were prepared and sealed in the glove box and removed for the experiments.

Results

Capacitance plots.—The location of the band energies is often estimated from Schottky-Mott plots of $1/C^2$ *vs.* V, where C is the capacitance of the semiconductor electrode (assumed to be the space charge capacitance) and V is the electrode potential. A typical plot for p-WSe_2 in a 0.1M TBAP/MeCN solution at 10 Hz and 10 kHz is shown in Fig. 1. This behavior was essentially unaffected by the addition of $PhNO_2$ to the solution. Analysis of the plot yields a flatband potential, V_{FB}, of 0.9V *vs.* SCE and a doping level of 4×10^{18} cm^{-3}. From this value and the bandgap energy, E_g of 1.4 eV, the location of the conduction and valence bandedge energies can be estimated, as shown in Fig. 2.

Cyclic voltammetry of various redox couples.—To study the effect of the redox couple in solution, on the behavior of p-WSe_2, the cyclic voltammetric (CV) response for a number of redox couples, in the dark and under illumination was investigated. The couples investigated and their standard potentials are shown in Fig. 2. From the location of the energy levels of these couples with respect to the bandedges, one would predict that a photocurrent for reduction could only be obtained for those with standard potentials in the range -0.4 to $+1.0$V *vs.* SCE (*e.g.*, TMPD/$TMPD^{+\cdot}$), if the "ideal" model of the interface applied (12). With this model, dark oxidation of the reduced forms of the couples with potentials above the conduction bandedge (< -0.4V *vs.* SCE), but not those in the gap, is expected. The experimental results for the different couples are summarized in Table I and details for some of these are discussed below. For TMPD (Fig. 3), a

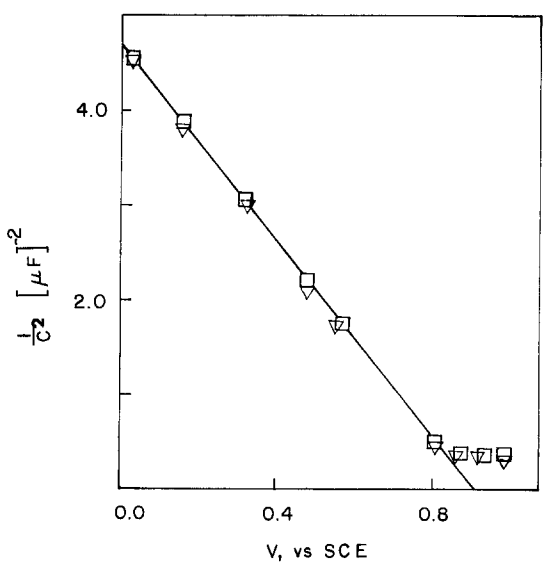

Fig. 1. Mott-Schottky plot of p-WSe_2 in MeCN containing 0.1M TBAP supporting electrolyte: (—□—□—) 10 kHz; (—▽—▽—) 10 Hz.

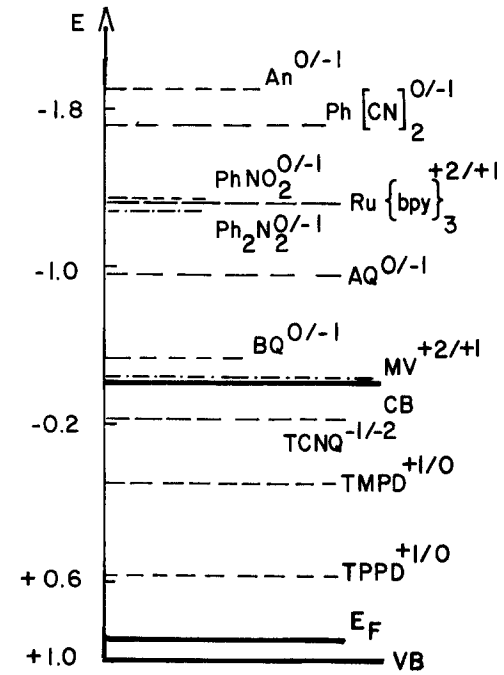

Fig. 2. Schematic representation of the energetic situation at p-WSe_2/solution interface along with V_{redox} of various redox couples investigated in this work. CB = conduction bandedge; E_F = Fermi level; VB = valence bandedge.

dark oxidation current is observed beginning at $\sim +0.2$V *vs.* SCE. The onset of photocurrent under chopped illumination, V_{on}, is $+0.55$V which is negative of V_{FB}. Similarly for TPPD, a dark two-step oxidation at potentials only slightly more positive than at Pt is observed and V_{on} for the small photocurrent is $+0.55$V. While these results are consistent with the usual semiconductor electrode model, with the presence of some surface states in the gap region accounting for the dark oxidation at energies above E_V, the behavior for couples above E_C requires the assumption of Fermi level pinning (13) or inversion (14). Consider the behavior of the $PhNO_2$ couple at p-WSe_2. The photoelectrochemical behavior was a function of both the con-

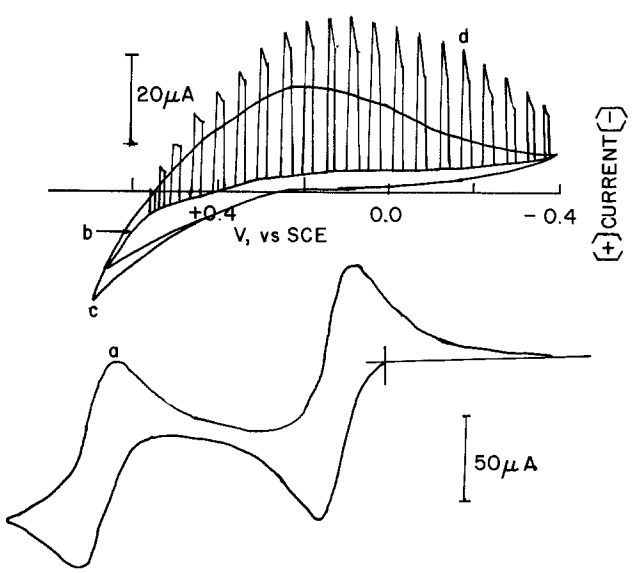

Fig. 3. Voltammetric curves on Pt and p-WSe_2 in MeCN solution containing 2.0 mM TMPD, 0.1M TBAP (supporting electrolyte). Light source 450W Xe lamp. Scan rate 20 mV/sec. (a) Cyclic voltammogram at Pt. (b) Dark voltammetric curve on p-WSe_2. (c) Voltammetric curve on p-WSe_2 under continuous illumination. (d) Current-potential characteristics under chopped light on p-WSe_2.

Table I. Voltammetric data and onset potential of photocurrent*

Redox couple**	V_{redox} (V *vs.* SCE)	V_{on} (V *vs.* SCE)	$V_{ph} = \lvert V_{redox} - V_{on} \rvert$
An(0/−1)	−1.90	−0.95	−0.95
$Ph(CN)_2$(0/−1)	−1.72	−0.85	−0.87
$PhNO_2$(0/−1)	−1.33	−0.40	−0.93
Ph_2N_2(0/−1)	−1.28	−0.34	−0.94
BQ(−1/−2)	−1.40	−0.44	−0.96
$Ru(bpy)_3$(+2/+1)	−1.30	−0.35	−0.95
AQ(0/−1)	−0.96	0.00	−0.96
BQ(0/−1)	−0.53	+0.38	−0.91
MV(+2/+1)	−0.43	+0.52	−0.95
TCNQ(0/−1)	−0.23	+0.54	−0.77
TMPD(+1/0)	+0.11	+0.53	−0.44
TPPD(+1/0)	+0.58	+0.55	−0.03

* V_{on} is defined as the potential at which 1% of maximal photocurrent is observed.

** Abbreviations: An = anthracene; $Ph(CN)_2$ = phthalonitrile; $PhNO_2$ = nitrobenzene; Ph_2N_2 = azobenzene BQ = benzoquinone; $Ru(bpy)_3$ = ruthenium 2,2′-bipyridine; AQ = anthraquinone; MV = methyl viologen; TCNQ = tetracyanoquinone dimethane; TMPD = N,N,N′,N′-tetramethyl-p-phenylene diamine; TPPD = N,N,N′,N′-tetraphenyl-p-phenylene diamine.

centration of $PhNO_2$ and that of $PhNO_2^{-\cdot}$. A cyclic voltammogram of $PhNO_2$ (0.2M) in MeCN at a Pt electrode (0.15 cm^2 area) (Fig. 4) shows the well-known wave for the reduction to the radical anion at −1.33V *vs.* SCE while only a small reduction current is found in the dark at p-WSe_2 (Fig. 4b); a small photocurrent is observed during the first scan (Fig. 4c). This photocurrent greatly increases during the second and subsequent scans under continuous illumination (Fig. 4d).

Clearly the presence of $PhNO_2^{-\cdot}$ in the solution greatly enhances the photocurrent for the reduction as illustrated in Fig. 5 where the effect of chopped illumination in a solution in which anion radicals were generated at the Pt electrode by the passage of 0.27 and 2.3C, is demonstrated. The effect of concentration of $PhNO_2^{-\cdot}$ (produced by electrogeneration) on the limiting cathodic photocurrent is shown in Fig. 6a. The photocurrent rises sharply at $PhNO_2^{-\cdot}$ concentrations up to 0.019 mM and then essentially levels off. The concentration of $PhNO_2^{-\cdot}$ at which this leveling off occurs depends somewhat on the $PhNO_2$ concentration. The magnitude of the maximum photocurrent at a given concentration of radical anion depends on the $PhNO_2$ concentration as shown in Fig. 6b. At low concentrations of $PhNO_2$, the current is limited by mass transfer of $PhNO_2$ to the electrode surface. At higher concentrations, the current saturates at a level governed by the light intensity. For irradiation with the full unfocused output of the 450W xenon lamp, this saturation occurred at ~0.2M $PhNO_2$. With $PhNO_2$ under these conditions, V_{on} was −0.4V *vs.* SCE; this represents reduction at potentials about 0.9V more positive than those at Pt.

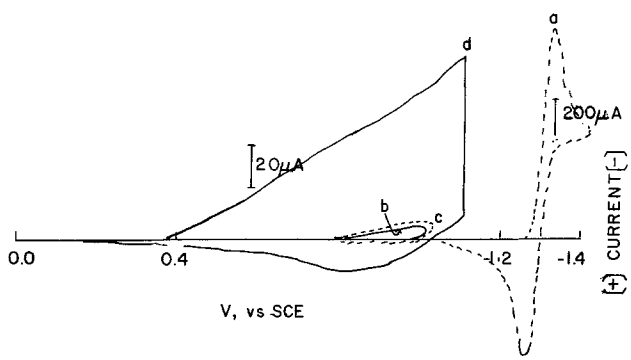

Fig. 4. Voltammetric curves of Pt and p-WSe_2 in MeCN solution containing 0.2M $PhNO_2$ and 0.1M TBAP supporting electrolyte. Scan rate 50 mV/sec. Light source, 2.0 mW He-Ne laser. (a) Cyclic voltammogram of the reduction of $PhNO_2$ at Pt. (b) Dark voltammetric curve on p-WSe_2. (c) Voltammetric curve on p-WSe_2 under continuous illumination. (d) Scan in continuous illumination after (c).

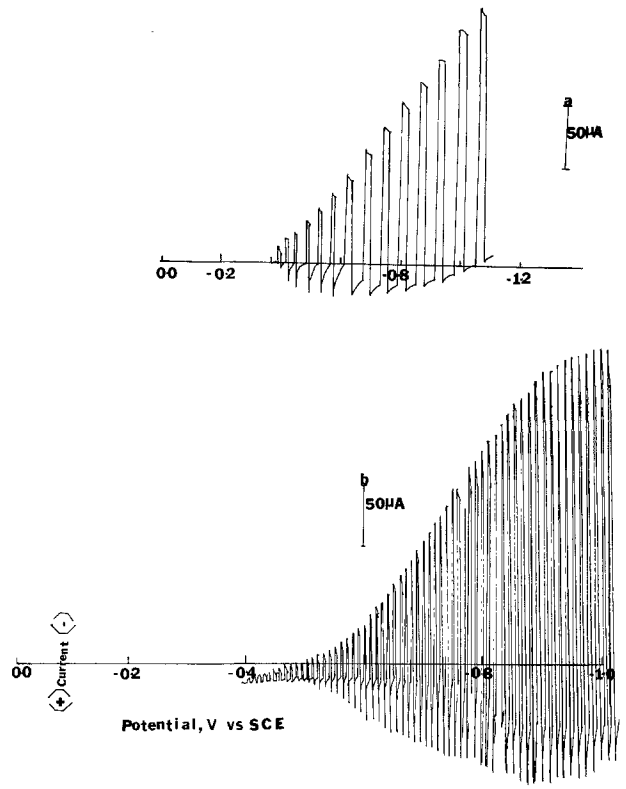

Fig. 5. Current-potential characteristics under chopped light on p-WSe_2 in MeCN containing 0.2M $PhNO_2$, 0.1M TBAP. Light source, 2.0 mW He-Ne laser. Scan rate 50 mV/sec. (a) After generating $PhNO_2^{-\cdot}$ electrochemically by passing 0.27C. (b) After generating $PhNO_2^{-\cdot}$ electrochemically by passing 2.30C.

For other couples with standard potentials corresponding to energies above E_C, similar photoeffects and underpotentials are observed (Table I). Note that with these V_{on} shifts more negative, as the standard potential becomes more negative so that the difference $V_{redox} - V_{on}$ is essentially constant at ~0.9V. Such behavior is characteristic of Fermi level pinning or in-

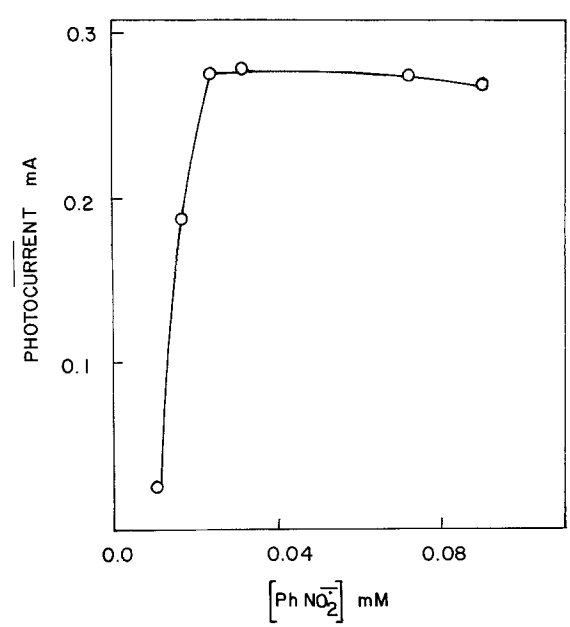

Fig. 6 a. Plot of photocurrent as a function of $PhNO_2^{-\cdot}$ in MeCN solution containing 0.2M $PhNO_2$ and 0.1M TBAP. Light source, 2.0 mW He-Ne laser.

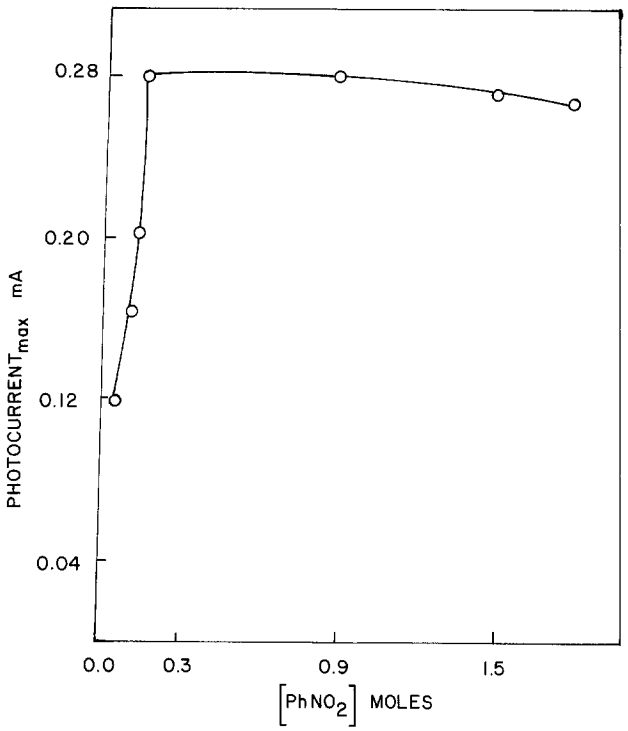

Fig. 6 b. Plot of maximum photocurrent vs. the concentration of $PhNO_2$ in MeCN. Light source 2.0 mW He-Ne laser. Supporting electrolyte, 0.1M TBAP.

version (13, 14). However, recall that couples at more positive potentials showed a relatively constant value for V_{on}, or a value of $V_{redox} - V_{on}$ which was a function of V_{redox}. The behavior for all the couples is illustrated in Fig. 7 and discussed below.

p-WSe_2/$PhNO_2$, MeCN solar cells.—A number of electrochemical photovoltaic cells based on nonaqueous electrolytes have been described (9). A general problem found with such cells for possible application to solar to electrical energy conversion is that the solubilities of the reduced or oxidized species in solution are low and mass transfer to either the semiconductor or counterelectrode limits the current at levels appreciably below those corresponding to the incident radiation. Since $PhNO_2$ can be mixed in all proportions, with MeCN, and as shown in Fig. 6, its concentration can be adjusted so that the saturation current is controlled by the light flux, photoelectrochemical cells of $PhNO_2$ and p-type semiconductors in nonaqueous solutions are particularly interesting. A two-electrode cell containing a p-WSe_2 photocathode and a Pt gauze (40 cm^2 area) counterelectrode immersed in an MeCN solution containing 0.2M $PhNO_2$ and 0.019 mmoles $PhNO_2^{\cdot}$ was fabricated. The *i-V* characteristics of such a cell obtained with different load resistances is shown in Fig. 8a. The open-circuit photovoltage was 0.56V and the short-circuit photocurrent was 0.11 mA. From this plot, the fill factor was computed to be 0.56. With this value of fill factor, the overall optical to electrical energy conversion was ~2.0%. The photocurrent as a function of time is shown in Fig. 9. The photocurrent was fairly stable for at least 3 hr, at which time the experiment was terminated. The relatively low efficiency of the cell suggests that recombination processes at the p-WSe_2 surface (*e.g.*, the oxidation of photogenerated $PhNO_2^{\cdot -}$) are important. Previous studies of n-WSe_2 have shown that exposed edges on the van der Waals surface of the electrode act as such recombination centers and that treatment with I^- or other halide ions appears to passivate these edges (1). Such an iodide treatment is also effective in improving the performance of the p-WSe_2 cell. If the p-WSe_2 electrode is immersed for ~45 sec in MeCN solution of 4 mM tetra-n-butylammonium iodide (TBAI), then removed, rinsed with MeCN, and immersed into the solar cell containing 0.2M $PhNO_2$ and 0.019 mM $PhNO_2^{\cdot -}$, a much higher photocurrent is observed (vide Fig. 8a). Although the V_{oc} and fill factor are essentially unchanged, this increase in i_{sc} increases the maximum power efficiency (monochromatic) to 4.1%. The effi-

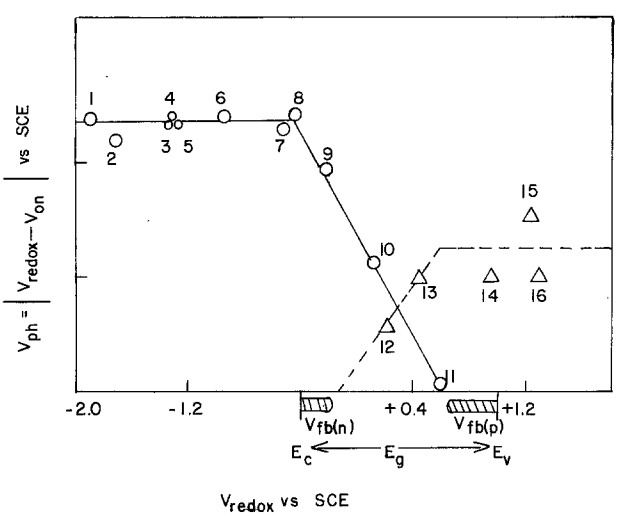

Fig. 7. Plot of $|V_{redox} - V_{on}|$ vs. V_{redox} for various redox couples employed in this study. 1 = Anthracene (0/−1); 2 = phthalonitrile (0/−1); 3 = nitrobenzene (0/−1); 4 = ruthenium 2,2'-bipyridine (+2/+1); 5 = azobenzene (0/−1); 6 = anthraquinone (0/−1); 7 = benzoquinone (0/−1); 8 = methyl viologen (+2/+1); 9 = tetracyanoquinone dimethane (+1/0); 10 = N,N,N',N'-tetramethyl-p-phenylene diamine (+1/0); 11 = N,N,N'N'-tetraphenyl-p-phenylene diamine (+1/0); 12 = iodide/iodine; 13 = bromide/bromine; 14 = chloride/chlorine; 15 = thianthrene (+1/0); 16 = ruthenium 2,2'-bipyridine (+3/+2). The values of V_{redox} and V_{on} for couples from 12 to 16 are taken from Ref. (1).

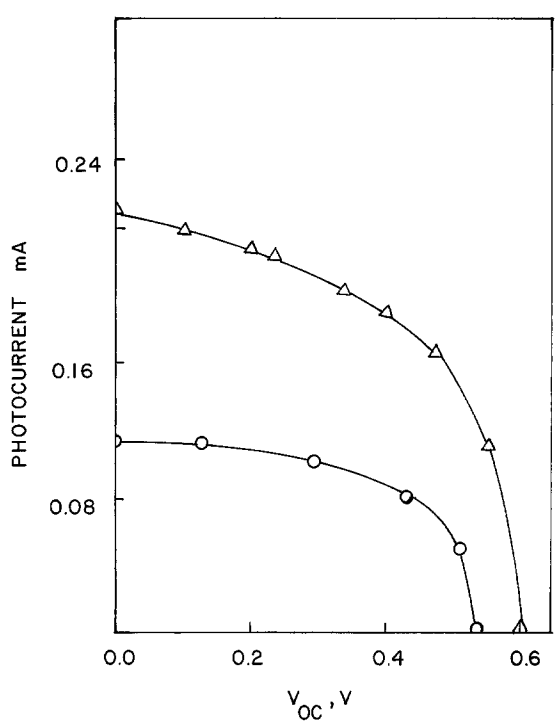

Fig. 8 a. Photocurrent-photovoltage characteristic of the cell p-WSe_2/MeCN, 0.2M $PhNO_2$, 0.019 mM $PhNO_2^{\cdot -}$/Pt. Irradiation source, 2.0 mW He-Ne laser. (—▽—▽—): The electrode was pretreated with 4 mM I^- in MeCN. (—○—○—): Not pretreated with iodide.

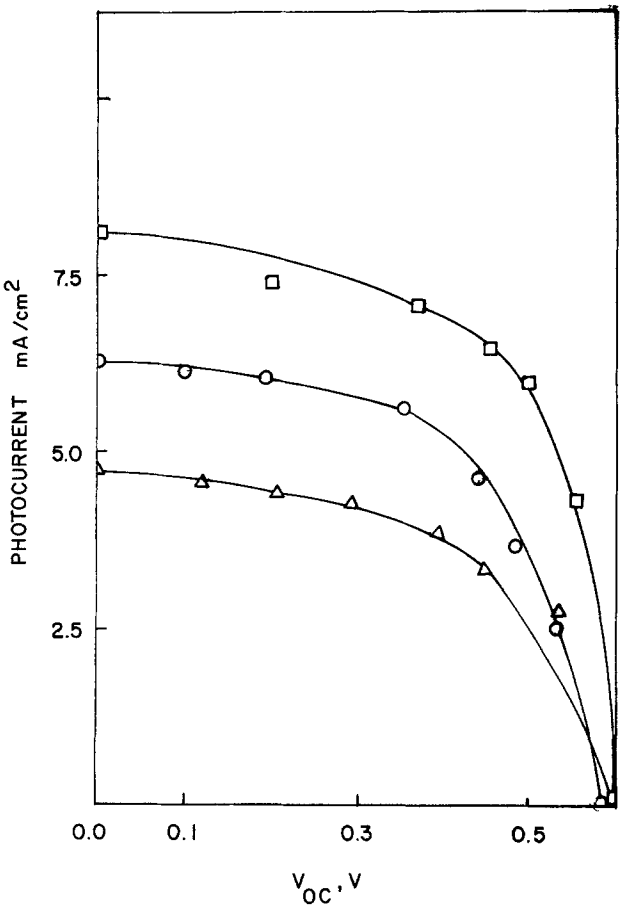

Fig. 8 b. Photocurrent-photovoltage characteristic of the cell p-WSe_2/MeCN, 0.2M $PhNO_2$, 0.02 mM $PhNO_2^{\cdot-}$/Pt. Irradiation sources: *(i)* 450W Xe lamp with 590 nm cut-on filter. (—□—□—): The electrode treated with 4 mM I^- in MeCN. (—△—△—): not treated with iodide. *(ii)* Direct sun: at Austin, Texas, around noon, in July 1980. (—○—○—): Treated with 4 mM I^- in MeCN.

ciency is similarly increased by the direct addition of 3 mM TBAI to the MeCN/$PhNO_2$ solution in the cell.

The behavior of the PEC cell was also studied at higher light intensities by irradiation with the red-filtered light of a 450W xenon lamp or by direct sunlight. The variation of photocurrent and photovoltage as a function of light intensity is plotted in Fig. 10 for a MeCN solution containing 0.2M $PhNO_2$ and 0.02 mM $PhNO_2^{\cdot-}$. The photovoltage and photocurrent increased sharply at low light intensities, but became essentially saturated at higher intensities. Essentially, the same behavior was observed for solution containing 2.0M $PhNO_2$/0.02 mM $PhNO_2^{\cdot-}$ (Fig. 10) which suggests that the saturation of photocurrent at higher light intensities was not caused by limited mass transfer of $PhNO_2$ to the electrode. Hence, the cause of the saturation of short-circuit current is probably recombination at the p-WSe_2 surface. However, treatment with iodide (as in the previous case) produced higher photocurrents and removed the saturation effect. This treatment caused little change in the open-circuit photovoltages. The overall behavior of the intensity of the PEC cell at maximum red-filtered xenon lamp and in sunlight is shown in Fig. 8b. Note that as with irradiation with the He-Ne laser, treatment of the p-WSe_2 with iodide produces a higher photocurrent with only a marginal increase of fill factor and V_{oc}. The overall optical-to-electrical energy efficiency in full sun is ~2% with the iodide-treated electrode.

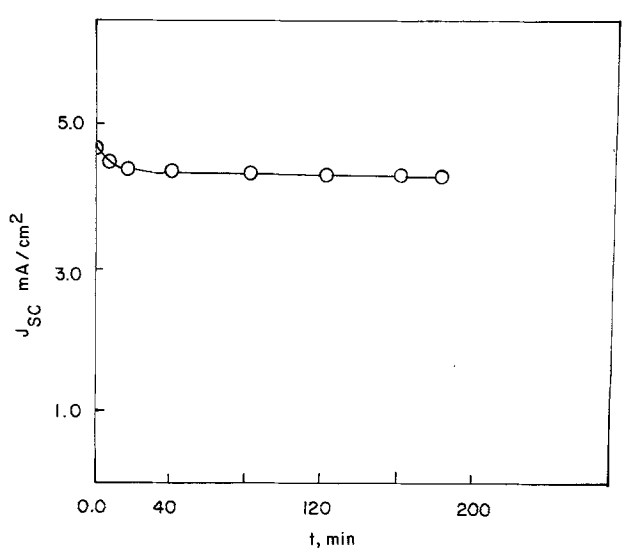

Fig. 9. Plot of photocurrent-output of the cell, p-WSe_2/MeCN, 0.2M $PhNO_2$, 0.02 mM $PhNO_2^{\cdot-}$/Pt as a function of time. Irradiation source: 450W Xe lamp fitted with 590 nm cut-on filter.

Discussion

The results of the photoelectrochemical experiments with the various redox couples, shown in Fig. 7, can be summarized as follows. The photopotential, V_{ph}, equal to $V_{redox} - V_{on}$, increases linearly with a slope near one, and then, at a potential near that corresponding to the conduction bandedge (~ −0.4V *vs.* SCE), it levels off at a constant value near 0.95V. Note that this parallels the behavior found with n-WSe_2/MeCN (1), except that for the n-type material the maximum photopotential was smaller (~0.5V) and that the leveling off occurred at potentials about 0.5V negative of the

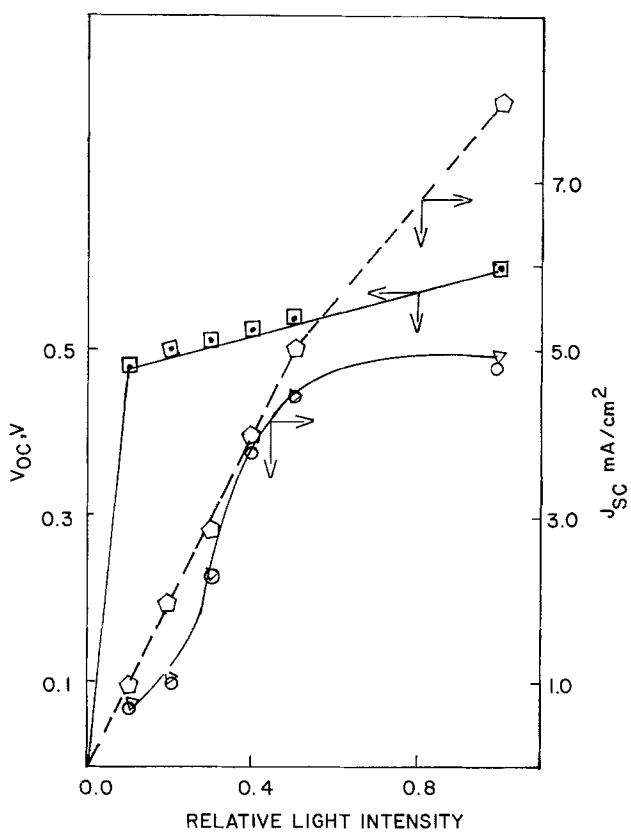

Fig. 10. Plot of V_{oc} and J_{sc} as a function of light intensity. Irradiation source 450W Xe lamp fitted with 590 nm cut-on filter. (—△—△—): 0.2M $PhNO_2$; 0.02 mM $PhNO_2^{\cdot-}$. (—○—○—): 2.0M $PhNO_2$; 0.02 mM $PhNO_2^{\cdot-}$. (⬡—⬡—): Treated with 4 mM I^- in MeCN. (—□—□—): Not treated with iodide. (—○—○—): Treated with 4 mM I^- in MeCN.

valence bandedge. The results with n-WSe_2 were consistent with the onset of Fermi level pinning (13) by surface states at energies about 0.5 eV above the valence band. The existence of such states as recombination centers could also explain the low values of V_{ph} found with p-WSe_2 for $TPPD^+$ (*i.e.*, the fact that the line V_{ph} *vs.* V intersects at +0.6V rather than at V_{FB} for p-WSe_2). The leveling at negative potentials for p-WSe_2 could be ascribed to pinning by surface states just below the conduction bandedge, E_C. Such states were invoked to explain recombination in n-WSe_2/MeCN (1). However, because the onset of this pinning occurs at a potential very close to the V_{FB} value of n-WSe_2 (*i.e.*, the conduction bandedge), the inversion model, proposed by Kautek and Gerischer (14) for n-type layered compounds could also apply. In both cases, the injection of electrons, either into surface states or at the surface at energies corresponding to E_C, causes the development of a negative surface charge which then causes changes in the potential drop across the Helmholtz layer. Thus, the pinning effect should occur in the presence of reductants of energies near or above E_C. Recall that the addition of $PhNO_2^-$ greatly promoted the photoreduction of $PhNO_2$ at WSe_2, in agreement with this concept. The effect of the introduction of a reduced form with a redox level energy above E_C to shift the bandedges has been seen previously, *e.g.*, in solvated electron production in liquid ammonia at p-GaAs (15), and with a number of couples at p-GaAs (16) and p-Si (17).

Acknowledgment

The support of this research by the Robert A. Welch Foundation and the Solar Energy Research Institute (in a cooperative project with SumX Corporation) is gratefully acknowledged.

Manuscript submitted Aug. 19, 1980; revised manuscript received Dec. 1, 1980.

Any discussion of this paper will appear in a Discussion Section to be published in the December 1981 JOURNAL. All discussions for the December 1981 Discussion Section should be submitted by Aug. 1, 1981.

Publication costs of this article were assisted by The University of Texas.

REFERENCES

1. H. S. White, F.-R. Fan, and A. J. Bard, *This Journal*, **128**, 1045 (1981).
2. (a) H. Tributsch, *Z. Naturforsch. Teil A*, **32**, 972 (1977); (b) H. Tributsch and J. C. Bennett, *J. Electroanal. Chem. Interfacial Electrochem.*, **81**, 97 (1977); (c) H. Tributsch, *Ber. Bunsenges. Phys. Chem.*, **81**, 361 (1977); (d) H. Tributsch, *ibid.*, **82**, 169 (1978); (e) H. Tributsch, *This Journal*, **125**, 1086 (1978); (f) H. Tributsch, H. Gerischer, C. Clemen, and E. Bucher, *Ber. Bunsenges. Phys. Chem.*, **83**, 655 (1979); (g) J. Gobrecht, H. Gerischer, and H. Tributsch, *This Journal*, **125**, 2085 (1978).
3. L. F. Schneemeyer and M. S. Wrighton, *J. Am. Chem. Soc.*, **101**, 6496 (1979).
4. L. F. Schneemeyer, M. S. Wrighton, A. Stacy, and M. J. Sienko, *Appl. Phys. Lett.*, **36**, 701 (1980).
5. L. F. Schneemeyer and M. S. Wrighton, *J. Am. Chem. Soc.*, Submitted.
6. F.-R. F. Fan, H. S. White, B. Wheeler, and A. J. Bard, *J. Am. Chem. Soc.*, **102**, 5142 (1980); *This Journal*, **127**, 518 (1980).
7. H. J. Lewerenz, A. Heller, and F. J. DiSalvo, *J. Am. Chem. Soc.*, **102**, 1877 (1980).
8. W. Kautek, H. Gerischer, and H. Tributsch, *Ber. Bunsenges. Phys. Chem.*, **83**, 1000 (1979).
9. P. A. Kohl and A. J. Bard, *This Journal*, **126**, 603 (1979), and references therein.
10. L. S. Marcoux, J. M. Fritsch, and R. N. Adams, *J. Am. Chem. So.*, **89**, 5766 (1967).
11. P. A. Kohl and A. J. Bard, *ibid.*, **99**, 753 (1977).
12. H. Gerischer, in "Physical Chemistry: an Advanced Treatise," H. Eyring, D. Henderson, and W. Jost, Editors, Vol. 9A, Academic Press, New York (1970).
13. A. J. Bard, A. B. Bocarsly, F.-R. F. Fan, E. G. Walton, and M. S. Wrighton, *J. Am. Chem. Soc.*, **102**, 3671 (1980).
14. W. Kautek and H. Gerischer, *This Journal*, In press.
15. R. E. Malpas, K. Itaya, and A. J. Bard, *J. Am. Chem. Soc.*, **101**, 2535 (1979).
16. F.-R. F. Fan and A. J. Bard, *ibid.*, **102**, 3677 (1980).
17. A. B. Bocarsly, D. C. Bookbinder, R. N. Dorniney, N. S. Lewis, and M. S. Wrighton, *ibid.*, **102**, 3683 (1980).

Technical Notes

Moderate Temperature Na Cells

II. Transition Metal Diselenide Cathodes

K. M. Abraham* and L. Pitts

EIC Laboratories, Incorporated, Newton, Massachusetts 02158

Recently we described (1) a moderate temperature rechargeable Na cell which operates at ~130°C and utilizes a β-Al_2O_3 solid electrolyte in conjunction with a transition metal disulfide cathode. In that study, we investigated the cathodic cycling behavior of TiS_2, VS_2, and $Nb_{1.1}S_2$. In our continuing search for suitable cathode materials for the moderate temperature Na cell (1-3), we have made a preliminary evaluation of the suitability of the diselenides, VSe_2 and $TiSe_2$ as rechargeable cathodes. Our findings are presented in this paper. While there have been prior studies dealing with the structural chemistry of the Na intercalates of $TiSe_2$ and VSe_2 (4, 5), very little is known about the reversibility of the intercalation reaction. The available data on the structural chemistry of the Na intercalates of $TiSe_2$ and VSe_2 show that structural changes of the host lattice occur with Na intercalation. An understanding of the effects of these structural changes on cathode rechargeabilities in Na cells is of both scientific and practical interest. Vanadium diselenide has been shown to be a highly reversible cathode in secondary Li cells utilizing nonaqueous solvents (6, 7).

* Electrochemical Society Active Member.
Key words: secondary cell, diselenide cathodes, sodium anode.